

Vibration Reduction of a Water Pipe T-Junction using CFD

Blake Eisner

University of Oklahoma School of Aerospace and
Mechanical Engineering
Norman, Oklahoma

Kurt Gramoll

University of Oklahoma School of Aerospace and
Mechanical Engineering
Norman, Oklahoma

Abstract---Pipe structure vibrations resulting from flow variations induced by displacement pumps can be problematic for hydraulic fracturing equipment. Multiple displacement pumps create a transient periodic flow velocity profile which is a function of the pump crankshaft phase. Pipe T-Junctions, used in hydraulic fracturing manifolds, with two inlets and one outlet combine the flow of two or more pumps. Research was conducted to study the coupling between flow variations from multiple displacement pumps and vibrations on a T-Junction. The research studied the effects of changing inlet flow phase and T-Junction flow geometry with the goal of reducing the mean and variant forces on the pipe structure. Research was done using transient commercial CFD simulations with fine mesh and a recently developed turbulence model, the Scale Adaptive Solutions (SAS) model. Thousands of time steps were used to model 1-2 periods of the flow output from a displacement pump. The mesh elements used were on the order of one million nodes. Inlet velocity and outlet static pressure boundary conditions were specified. The forces of interest were in the two directions along the axis of the orthogonal pipes and they were calculated by adding the total force exerted on the walls of the structure with the force caused by the static pressure at the inlets and outlets. Changes to the flow geometry included a fixed orifice, helix causing rotating flow, an expansion chamber and a cone shape. The expansion chamber geometry study showed a significant reduction in the forces exerted in the transverse direction and the results showed it was the most favorable geometry for both flow input velocity profiles.

Keywords—T-Junction; Vibration; Manifold; CFD; SAS; turbulence; displacement pumps;

I. INTRODUCTION

A fracturing manifold typically consist of a semi-truck trailer with two to three large diameter pipes (diameter usually greater than 4 in) running down the length of the trailer. Five pumps could be connected on each side of the unit for a total of 10 pumps. It is not uncommon to have more pumps adding to the flow in a ground manifold upstream of the wellhead. Water and sand travel from the water and sand trucks to the blender where it is mixed into slurry and pumped, generally with a centrifugal pump, to the low pressure side of the manifold. This low pressure slurry travels from the manifold to well service pumps (fracturing pumps) where the fluid pressure can be raised to as high as 15,000 psi (103.42 Mpa). From the fracturing pump it travels back to the high pressure side of the manifold where the flows are combined into large pipes that run the length

of the trailer. High pressure fluid exits the manifold trailer at the front and travels through pipes assembled on the ground to the wellhead.

An important area of concern is the manifold since it is exposed to vibrations resulting from the flow variations from the fracturing pumps. It is not uncommon for manifolds to experience high loads or vibrations that cause part failures. Thus, research in reducing vibration of the manifold was needed.

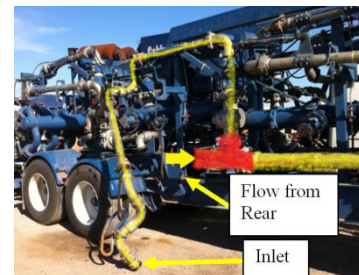


Fig.1. Articulating Frac Arm Manifold Trailer (AFAM)

A recent manifold, the AFAM, is shown in Figure 4. The yellow line highlights the path the fracturing slurry takes coming from the high pressure output of a pump. A possible area of high vibration is the T-Joint where the flow is combined to one pipe (shown in red).

Forces causing vibrations in the manifold come from two different sources. First, some of the forces are transferred through the walls of the pipe structure from the fracturing pumps. Swivel joints are used in the piping structure to help mitigate the force traveling through the wall of the structure. A swivel joint allows for movement of the pipe structure by allowing rotation of a ball bearing containing joint. Combining a number of rotational joints with pipe elbows allows for translational and rotational motion. This helps to reduce the vibrations transferred through the pipe walls. The second major source of vibration comes from the dynamic fluid flow interaction with the walls of the structure. Dynamic fluid flow causes forces on the walls in the form of both static and dynamic pressure. This research focused on the fluid interaction with the wall of the pipe as the vibration source and explores methods of reducing it. Specifically the pipe structure T-Junction highlighted in red previously was the focus of the research. This part of the

manifold was chosen as it was thought to be a major contributor to the vibrations of the entire structure.

The configuration of the fluid volume used for the study is shown in Figure 6 which corresponds to a simple T-Junction used on manifolds. The interest lies in either finding a change to the flow geometry that reduces vibrations. Changing the flow geometry comes with restrictions. Any change made to the flow geometry must have a conceivable way of manufacturing the part. It also should not occupy a significant amount of space. Any part made would still need to fit onto a trailer that has both weight and space restrictions. Simply making all parts larger is not an option. Ideally, any change made would either take away a minimal amount of material or be an addition of a part.

Field observations showed that placing a fixed orifice (henceforth known as a choke), in the line just before the vertical line attached to the horizontal collection line, reduced vibration in the manifold. The flow direction is shown by the arrows. The choke is circled yellow in Fig.2. This is an example of a feasible change to the geometry because it could be achieved by inserting a choke into an existing configuration.

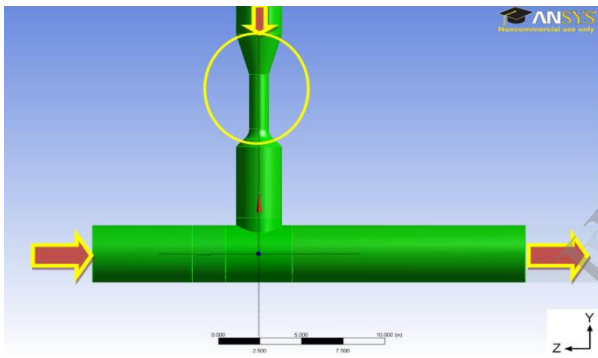


Fig.2.Fluid Volume Setup

One of the goals of the research was to try and verify the field observations that the addition of the choke reduced the vibration forces on the structure using CFD. If the simulations showed a reduction in vibrations the design was to be optimized. As is discussed in detail later, it was found that the largest vibration forces were found to be in the Y and Z-Directions. The forces were split into these two orthogonal components. The Z-Direction runs down the length of the trailer. All of the figures show the orientation of the parts if one was looking at the side of the trailer. Forces in this direction are aligned down the axis of the large diameter pipe and result in tension or compression of the pipe. Forces in the Y-Direction are transverse to the length of the trailer. As such they create bending loads on the unit which were thought to be more detrimental. For this reason, reducing the force in the Y-Direction was the main focus of the study but the Z-Direction forces was still examined. Other fluid geometries that were thought to be effective were explored and are shown summarized in Fig.3. Note that the figure just gives a summary of the geometries for reference and they are not to scale. The exact

dimensions of the configurations can be found in the full research thesis [1]. The choke geometry was varied by changing the distance from the trailing edge of the choke to the center of the horizontal pipe. It is expressed in terms of choke lengths in the results.

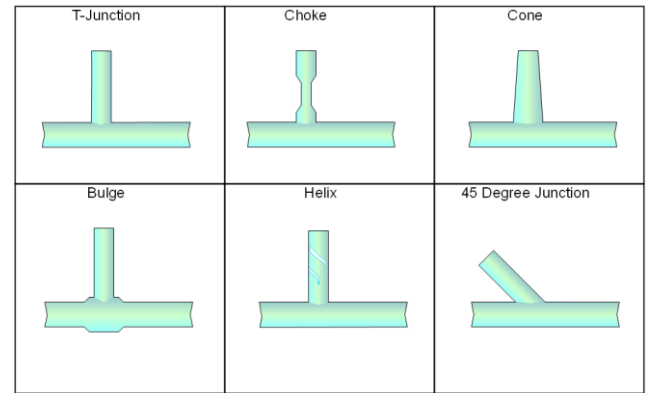


Fig.3. Fluid Geometry Summary

It was mentioned earlier that the energy needed to fracture rock comes from the pressure and flow rate created by the pumps. The transient output flow from the fracturing pumps is the cause of the fluctuating forces exerted on the pipe that this research examined. As such, the flow profile needs examining as it was an input of the study. Fig.4 shows an example of a piston displacement pump. The slider crank mechanism of the pumps can be used to find the flow output with respect to the crankshaft position.

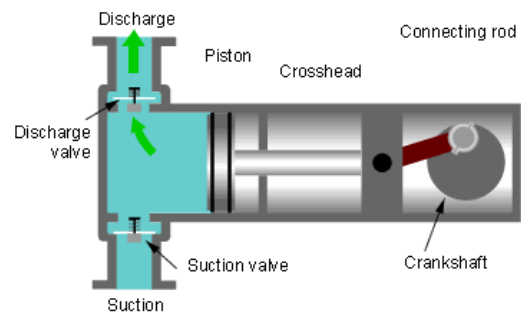


Fig.4.Positive Displacement Pump [2]

As a result of the high pressure and flow rate needed to fracture a rock formation, a number (10+) of reciprocating plunger pumps with power inputs as high as 3000 hp(2237 kw) can be used in parallel to meet the flow parameters required for the formation. One drawback of using reciprocating pumps is that the discharge flow rate from the pump is not constant. Figure 9 shows the combined flow output of two triplex reciprocating pumps (three cylinders) running with their crankshaft positions In-Phase (IP). The example has an 8 inch plunger diameter and a stroke length of 12 in (0.3048 m). The flow varies up to $\pm 9.4\%$ from the average flow rate. The pump speed used in the study was 180 rpm. When the flow of two similar pumps flow are combined In-Phase, the percentage of maximum flow variation from the average does not change, but the value

of the variation doubles to 28.3 gal/min (1.785 l/s). This was shown by the "Total Flow Both Pumps Curve." If a pump with more cylinders such as a quintuplex pump is used, the flow variation decreases. Note Fig.5 gives an approximation of the pump discharge. It may be affected by valve efficiency and the ratio between the connecting rods to the crankshaft radius. These factors were neglected in order to simplify the flow and try to remove the connection to specific pumps. Using the exact pump flow output would require choosing a specific pump model. The In-Phase flow serves as a worst case scenario for the flow. The section of the curve between the two yellow lines is referenced to as one flow cycle.

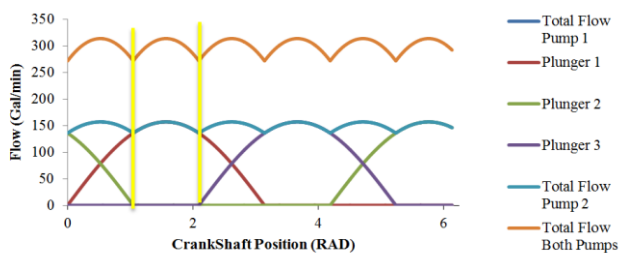


Fig.5. Flow vs. Crank Shaft Position for Two Triplex

This research is important to the Oil and Gas industry because excessive vibration forces can result in fatiguing and eventual failure of equipment. Part failure creates a substantial monetary cost resulting from replacing broken equipment and down time. In addition, workers may be close to equipment when it fails. Since the parts contain such high pressure, failure may lead to injury and possibly loss of life. Reducing the vibrations likely translates to reduced equipment failure. The research helps to understand the exact parameters that influence the vibration forces. This could help define future design constraints. The vibrations had to first be understood before they could be combated. Thus there is a section which examines the forces on the structure resulting from the flow and the turbulent models needed to simulate the flow.

The objective of the research was to determine whether or not it was possible to reduce flow induced vibrations in a T-Junction by inserting an orifice into the flow using Computational Fluid Dynamics (CFD) simulations. Based upon field observations, the fixed orifice reduces vibrations on the T-Junction. The effectiveness of the fixed orifice was studied by varying its distance from the main line. Other geometries thought to reduce vibrations more effectively were also explored. Only minor changes in geometry were used because the part would have to be placed on a trailer if it were to go to production. Large changes to the geometry may violate the weight and space restrictions of the trailer and thus would not be feasible. Data resulting from this study may allow companies to make changes to part geometries that would be both feasible from a manufacturing standpoint and may create a competitive edge to their products. The CFD models used were the most accurate and complete ones available with the technology readily available at the time

of the study. The mesh size in the areas though to have the highest velocity gradients was 0.0984 in. The highly detailed mesh resulted in a node count used was around one million and about one thousand time steps were used for each flow cycle. The high element count allowed the high end SAS turbulence model to be used. The goal was to try and reduce pipe vibrations as much as possible by either making small changes to the geometry. Additionally, a better understanding of the nature of the resulting forces and what parameters of the flow caused them was found.

The T-Junction shown in Fig.3 was the only part of the flow structure modeled. Studying the T-Junction only allowed direct cause and effect of a relatively simple geometry changes that could be analyzed. Furthermore, limiting the geometry to a small region allowed for a high ratio of the flow length scale to the mesh size. This also made it possible to use the most accurate but computationally expensive turbulence models possible with today's technology. The CFD models output the force exerted on the walls. The force on the walls added to the pressure force on the inlets and outlets was taken as the total force output on the structure and was used to compare different geometries.

II.BACKGROUND

It is common to see piping failure in cases where the flow pulsations coincided with the natural frequencies of the piping structure which can amplify the vibration on the system by up to 800 times. Dampers can be effective at damping out acoustic pulsations, which travel at the speed of sound in the fluid. Generally, well service pump have output flow pulsations of less than 15-20 Hz. Reciprocating pumps generate pulsations at integer multiples of its operating frequency, but the higher the frequency multiplier the lower the amplitude of the force [3].

Placing a choke in the piping system acts as a resistive, or pressure drop device. However, placing a choke at the discharge of a displacement pump causes the static pressure to rise upstream of the choke. This raised the overall pressure of the system which may be problematic. This type of damper is said to be most effective at damping high frequency modes [3]. This study assumed that the higher frequency modes were of negligible magnitude compared to the forces induced at the pump frequency and thus the higher frequency modes were ignored. Though it should not be ignored that higher frequency pulsations could make a significant contribution to the forces if they were close to the natural frequencies of the system. Unfortunately, the common designs for pulsation dampers used volumes to help attenuate the pulsations. The objective was to not severely influence the flow geometry, so these concepts were not feasible.

It has long been observed that there are preferred pipe junction arrangements to help prevent vibrations from occurring. These are laid out in handbooks and articles such as in [4]. The flow arrangement of the junction being examined matched with the Typical T. Ideally the junction would be angled. This is shown in the preferred

arrangement, but other design constraints make this not realistic in many cases.

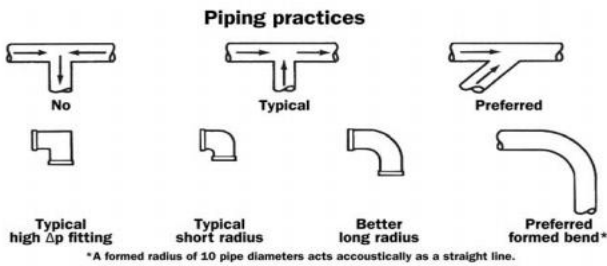


Fig.6.Best Piping Practices [4]

Due to the competitive nature of the oil industry, a large amount of the studies and research conducted around the field of pipe vibration is funded by companies. As such, research previously conducted may not have been made available to the public and was kept as proprietary. There might have been more information and research that has been conducted in the private sector which is not public information.

III. GEOMETRY SETUP AND MESHING

The initial T-Junction geometry used came from existing designs used in fracturing manifolds. Initial choke experimentation was driven by observations that placing the choke in the flow, close to where the pipes are combined, helps to reduce vibrations. The information of the exact spacing from the main lines was not available, so different spacing increments were used. Fig7 shows the general flow geometry used. Note that all geometry modeled is the flow geometry, not the solid pipe wall. The horizontal pipe parallel with the Z-Axis has a diameter of 4 inches and will be known as the main or large line. The vertical pipe aligned with the Y-Axis had a diameter of 2.75 in (0.06985 m). The direction of the flow is indicated by the arrows. The inlets on the 2.75 in. (0.06985 m) and 4 in. (0.1016 m) pipes shall henceforth be known as the small and large inlets respectively. The portion shown in gray shall be known as the T-Part.

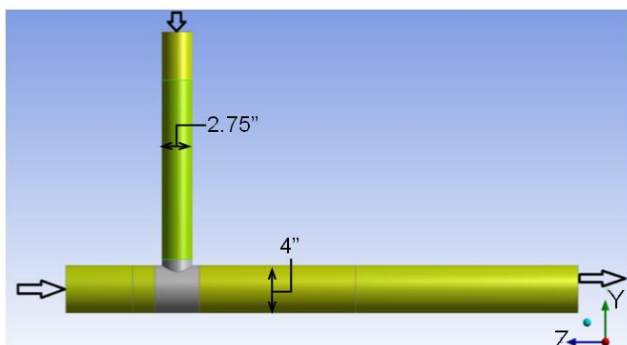


Fig7.T-Joint Geometry

Since one of the desired outputs was the force on the walls of the structure, it was important to have a refined mesh near the walls. Wall inflation was used in an attempt to make the near wall region more accurate. An assumption

made was that pressure forces would dominate the vibrations of the structure. Exact modeling of the viscous region was not paramount. Moreover, resolving the near wall region would require the first layer height to be decreased by 1-2 orders of magnitude (resolving the near wall region required the y^+ value to be about 1). To avoid highly elongated cells, the other dimensions of the cells would have had to be reduced as well. This would greatly increase the mesh count near the wall. Any y^+ value of 140 it was found that the first layer height needed to be 0.015 in. The value of y^+ was chosen because it was in the acceptable range given by ANSYS and the assumption that the viscous sub layer would not substantially affect the results.

The inflation was controlled using the first layer height and the total number of inflation layers which was set to 12. The growth rate of the mesh layers was set to 1.03 to ensure a small change in the volume of the elements in the direction perpendicular to the walls.

The final meshing of the T-Part contained 153,583 nodes and 586,363 elements with a maximum skewness of 0.82. The T-Part was made small to reduce the number of tetrahedral cells in the overall geometry as they were not as desirable as the swept element types.

All straight pipe sections were meshed using a swept mesh with a max element size of 0.0984 in. (0.00249 m) for the parts sharing a face with the T-Part. The source of the sweep was the face shared with the T-Part. In other words, the mesh on the respected face of the T-Part was extruded to form the swept mesh. This type of mesh required the T-Part to be meshed first as every subsequent mesh was determined by it.

The sections farthest away from the T-Part, highlighted green in Fig.8, were meshed using a sweep with the same target settings. The only difference was the maximum face size was allowed to be twice that of the T-Part, 0.197 in. (0.005 m). This was done because it was assumed that the flow had either been fully developed or was close enough that it would not significantly affect the force output on the structure.

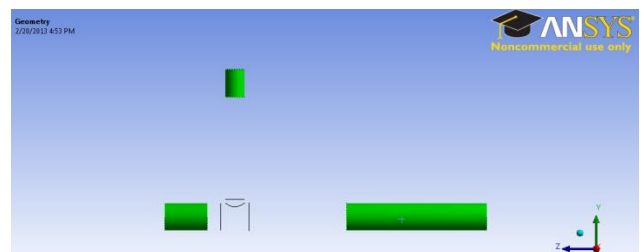


Fig.8.Final Meshed Sections

The total node and element count for the entire mesh was 1,085,882 and 1,846,199 respectively. The maximum skewness was the same as that of the T-part, 0.82. This same meshing strategy was used on all of the different

geometry configurations. The only differences came from the local geometry unique to the different configuration

IV. FORCE FORMULATION

The outputs of FLUENT were the forces on the wall of the structure and the static pressure at the inlets. These were recorded for every time step. The wall force was calculated by FLUENT by summing the force across all nodes that laid on the walls. This was done separately for each of the three coordinate directions. The average of the static pressures at both of the inlets was area weighted. In order to get a complete picture of the forces on the entire structure, the forces resulting from the pressure at the inlets was added to the force on the wall. This resulted in the total force on the structure being calculated using

$$F_y = F_{yw} + A_s p_s \quad (1)$$

where F_{yw} was the force on the walls in the Y-Direction A_s was the area of the small inlet and p_s was the static pressure on the small inlet. Likewise,

$$F_z = F_{zw} + A_l(p_l - p_o) \quad (2)$$

gave the total force on the structure for the Z-Direction. A_l was the area of the large inlet, which was the same area as the outlet, p_l was the static pressure of the large inlet and p_o was the static pressure at the outlet which was constant. Fig.9 shows a diagram of the force calculations. F_{yw} and F_{zw} were calculated on the walls of the pipe structure, shown orange in the figure, in their respected directions. FLUENT output the sign wall force terms with the direction taken into account. The force in the X-Direction (into the page) did not require any inlet or outlet pressures to be taken into account because there were no inlets or outlets lying in this direction.

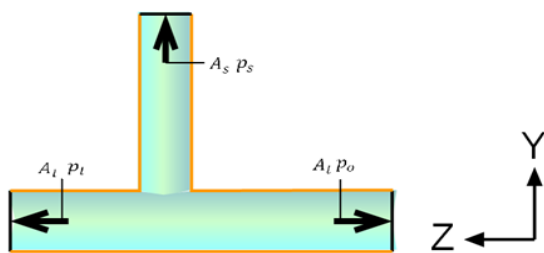


Fig.9. Force Calculations

Total force data was available for each of the Cartesian coordinate directions corresponding to a time step. In attempt to reduce the forces over an entire cycle to one value that could be easily compared, the mean was taken of the force over the time steps recorded. This was taken over two flow cycles for the studies. The mean force was important for understanding the effect of a change in geometry, but did not correspond to vibration. Since reducing vibration was the main goal of the research, the maximum variance from the mean was calculated for each

study. This produced a single force value for each study in each of the coordinate directions that was taken to be the most important parameter in vibrations. This essentially gave the amplitude of the force profile and gave a result that could be a parameter for product design.

V. CFD SETTINGS

The solver used was a transient pressure based solver for incompressible flow. The only output of interest was the force on the walls of the pipe structure and the static pressure at the inlets. For this reason the only model used was a turbulence model. The fluid used for the study was water with a density of 62.31 lbm/ft^3 (998.1 kg/m^3) and a viscosity $6.739 \times 10^{-4} \frac{\text{lbm}}{\text{ft}\cdot\text{s}}$ ($0.001 \frac{\text{g}}{\text{m}\cdot\text{s}}$).

TABLE1. Reynolds Numbers for Pipe Section Geometries

Pipe Section	Reynolds Number Range (10^5)
Inlet small	6-7
Inlet Large	6.7-10.2
Outlet	12.9-15

All of the flow was fully turbulent for the entire domain as is shown in TABLE1. The transient flow velocity and the mixing of the two pipe flows also promoted turbulence. The SAS (Scale Adaptive Solution) turbulence model was used to model all of the flows. The flow became fully transient when using this model type; no steady state solution existed. The curvature correction was not used and all model constants were left at their default values.

Fig.10 showed two representative images of velocity magnitude for the T-Junction along the symmetry axis of the structure. The top image showed the k-e model time averaged out the flow throughout the domain. This resulted in a steady state solution. The SAS model showed the unsteady nature of the flow and did not yield a steady state solution.

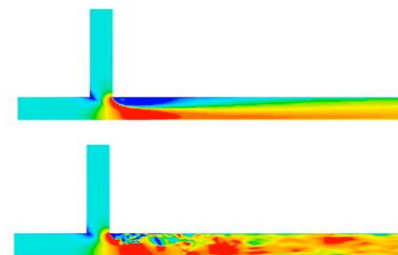


Fig.10. Velocity Magnitude of k-e (top) and SAS (bottom) Turbulence Model

The SAS turbulence model was the most comprehensive model that could be chosen for the computational resources available at the time of the simulations. It was intended to model the flow in the most accurate manner possible in attempt to capture the overall flow behavior at the smallest scales the resources allowed. Of course models only allow a portion of the spectrum to be represented but it was assumed that only the large scales

(size of the mesh or larger) would contribute significantly to the mean flow. The turbulence model was the only flow model used. It was assumed that other models (acoustics, energy etc.) would not contribute to the flow parameters of interest.

A. Boundary Conditions, Outputs and Solver Settings

The outlet was set to a pressure outlet with a static pressure of 15,000 psi (103.42 Mpa). This pressure was used as a reference to the highest hydraulic fracturing pressures generally used in industry. Using this high pressure gave results reflecting actual pressures that may be seen in the parts. This allowed the maximum probable pressures to be recovered. However, the outlet pressure for the simulation did not influence the results. The results from this study would have been unchanged if the outlet pressure was set to 0 because the flow was incompressible.

The outlet turbulence settings were specified using backflow hydraulic diameter and turbulent viscosity. The turbulent intensity was taken to be 5%. It was originally assumed that pressure forces would dominate the total vibration of the part. From this it was assumed that the regions of the domain that only had straight pipe flow (next to inlets and outlets) would not significantly add to the forces of the structure.

The velocity input was specified using an interpreted UDF (User Defined Function). This allowed the velocity profile to be a function of the flow time which translated to crankshaft position and angular velocity. The input velocity is shown graphically in Fig.5 in the Introduction as well as overlaid on figures in the results.

The walls were set to stationary walls for the entire flow boundary. The only shear conditions used was the no slip boundary condition. The wall roughness cannot be specified when using the SAS turbulence model; the model ran solely off of the no slip condition.

The coefficient of drag was recorded for each time step of the calculation and was output in each of the three Cartesian coordinate directions. The coefficient of drag was used to find the force on the walls of the pipe.

The static pressure at the inlets was needed to find the force being outputted on the structure. It was found using an area-weighted average of static pressure on the large and small inlet faces.

Studies seemed to converge the quickest and were the most stable when a SIMPLE (Semi-Implicit Method of Pressure-Linked Equations) was used. The gradient was calculated using the Green-Gauss Cell Based Method. The pressure scheme used was the PRESTO! (PREssureStaggering Option). The momentum, turbulent kinetic energy and specific dissipation rate all used first order upwind schemes. The transient formulation used a bounded second order implicit scheme.

The solution control under-relaxation factors were generally reduced to low values (<0.5) until convergence was achieved for the first few time steps. The calculation was then stopped and the controls were returned to their default values. This was done to increase the performance of the solver and reduce the time it took to converge to a solution. The higher order terms were relaxed for all variables using a relaxation factor of 0.75. Double precision was used for all studies.

Convergence was monitored by checking the residual values for the continuity, x-velocity, y-velocity, z-velocity, k and ω . The criteria for convergence was left to the default value of 0.001. All residuals did converge monotonically.

VI. RESULTS

Fig.11 shows that there was little difference between the force plots of the different trials in the Z-Direction. It was difficult to distinguish between the different trials. Any differences between geometries was negligible. The velocity profile for both of the inlets was overlaid on the chart to help give context of the forces.

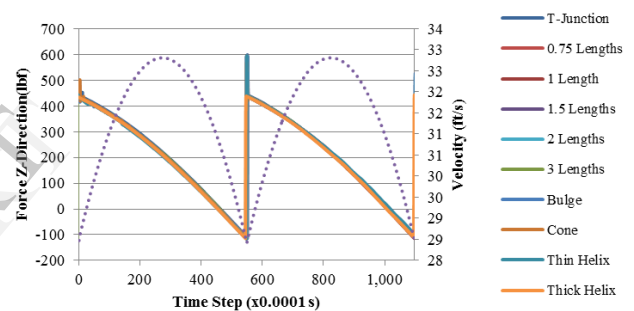


Fig.11. Z-Direction Force Summary

Fig.12 gives two views of the force calculation results. The difference between the trial with the largest mean and the smallest was only 3 lbf (13.3 N). This was less than a 2% difference. It was assumed that any minute difference could be ignored or attributed to error. Even if the value was of physical significance, it would not be enough to make a real world difference. The same could be said about the maximum variance. The difference in variance was larger, 8 lbf (35.5 N) from the highest to the lowest, a difference of 3.7%. This was taken to be an inconsequential amount. Thus the results showed that the changes made did not show any impact on the forces in the Z-Direction.

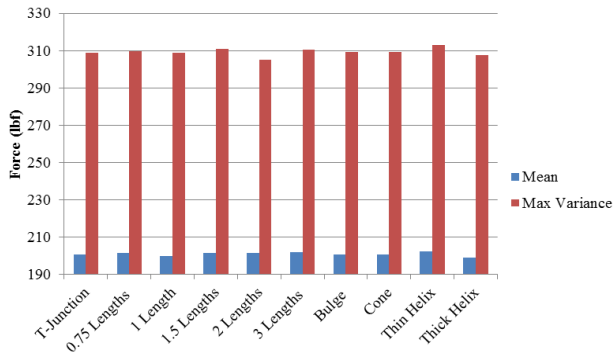


Fig.12.Z-Direction Force Summary

The forces in the Y-Direction were affected noticeably by the differences in flow geometry as can be seen in Fig.13. The choke trials had higher force magnitudes than the base line T-Junction for all flow times. It first appeared that the force approached ~-10lbf (44.5 N) around time step 275 for the choke, T-Junction and bulge trials. This was the location where the time derivative of the velocity inlets approached zero. The cone stood apart from the other trials. Its force was less the baseline for all time steps and less than the chokes that were closer than 1.5 lengths.

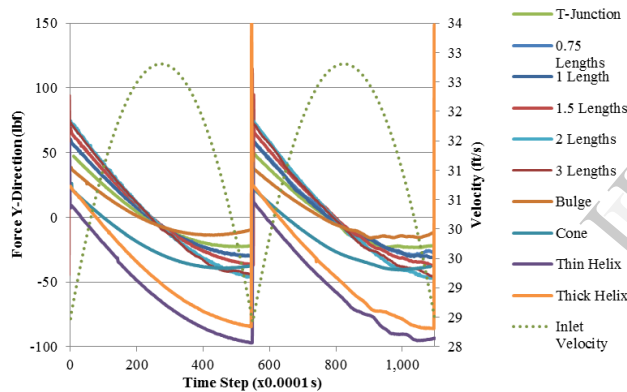


Fig.13. Y-Direction Force Summary

Fig.14made it easy to quantitatively compare the different trials. The T-Junction, all of the choke trials and the bulge had mean values that were essentially 0 lbf. All of the choke trials had larger variance, a minimum of 20% higher, than the baseline. The Helix design did not show favorable results. They both had average absolute force values far larger than the base line and had large variances. The thin and thick helix had variance 126% and 36% higher than the baseline respectfully. The bulge and the cone both had encouraging results. The cone had a mean force magnitude 21 lbf (93.4 N) higher than the base line, but the variance was 2 lbf (8.9 N) less, a modest decrease of 4%. The bulge had the best results of all the trials with a mean force of 0 lbf and a variance 11 lbf (48.9 N) less than the base line. This was a decrease of 22%. This was a physically significant amount.

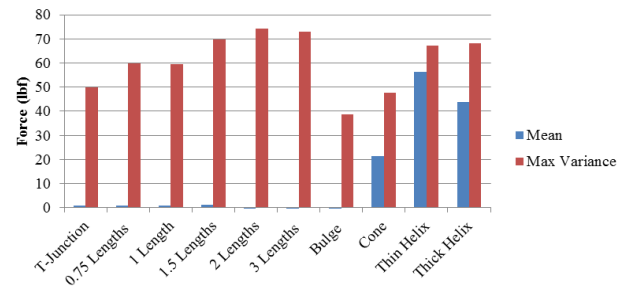


Fig.14. Y-Direction Force Summary Chart

VII. FORCE EXAMINATION

The results from the studies showed an interesting phenomenon. They appeared to have a discontinuous jump in the force of the structure in both the Y and the Z-Directions that occurred at around time step 550. It originally did not seem reasonable that this type of force behavior would be caused by a continuously changing velocity profile. A side study was conducted with interest in finding if the jump in the forces had a physical significance or was it caused by an instability in the numerical scheme.

In attempt to remove the jump, a parabola was fitted to the velocity profile, which is shown in Fig.15. The addition of the parabola to the velocity profile removed the jump and replaced it with what appeared to be a linear function. This was interesting because the derivative of a parabolic function was a linear function. This suggests that the force exerted on the T-Junction is related to the time derivative of the inlet velocity profiles. This implied that the force jump seen in the results was due to the change in the sign of the derivative of the velocity input which gave a physical significance.

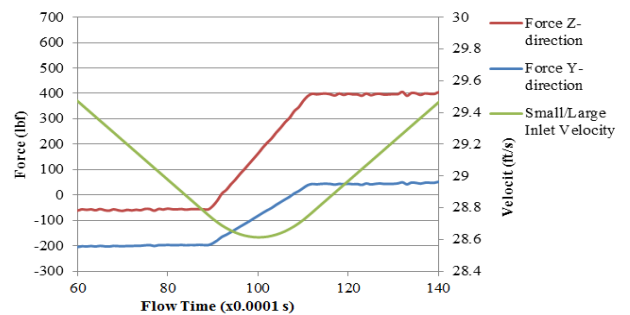


Fig.15.Parabola Velocity Input Profile

VIII. CONCLUSIONS

It is interesting to note that for the studies, favorable results are only obtained from the flow geometries that increased the flow volume domain (cone, bulge). The trials that took away from the fluid domain (choke, helix) increased the vibrations. The results also show the choke that is being used in the field is not the most effective, as it actually showed an increase in forces on the T-Junction. It should be noted that it is possible the choke reduces vibrations on the manifold by changing some parameter of the system not in the scope of the study.

It appeared that the change in linear momentum of the fluid did not play a huge role on the vibration. The force caused by the changing of the momentum was much smaller than the force resulting from the pressure at the inlets.

The trials that show the best results had not been optimized in any way. The geometry and results shown for the cone and the bulge were the first design iterations of the concept. They were design under the premise of changing the geometry and removing the least amount of material as possible. It was possible that making minor geometry changes to the trials shown to be effective could make them more favorable. Optimizing these two designs would be a possible area of future research.

It may give interesting result to try and combat the forces in the Z-Direction by placing a choke or a cone type design in the main line. The results showed that there were some distinct advantages in having flow inputs that are Out-of-Phase. If these results could be verified experimentally, highest amount of vibration reduction may be achieved by controlling the phase of the pump crankshafts.

This study provided an interesting application where CFD may be the only way to get results for this application. Experimental results would be difficult to obtain because of the nature of a thick walled pipe structure. It would be difficult to isolate the forces induced on a T-Junction by the fluid from the forces traveling through the walls of the pipes from other areas in the system. In the field there would also be a number of T-Junctions attached to the same structure causing forces that may produce noise on the T-Junction of interest. For these reasons it may be difficult to record valid experimental data to validate a CFD model.

REFERENCES

- [1] Eisner, B. R. (2013). Vibration Reduction of Water Pipe T-Junction Using CFD. Norman: University of Oklahoma.
- [2] Commonwealth of Australia. (2012, March 25). Chemical and Oil Refining. Retrieved April 6, 2013, from Toolboxes: <http://toolboxes.flexiblelearning.net.au/demosites/series2/204v2/PROC201/PROC201-010100-RecognisePumps.htm>
- [3] Engineering Dynamics Incorporated. (1988). Understanding How Pulsation Accumulators Work. (E. Seiders, Ed.) Pipeline Engineering Symposium- PD-Vol. 14.
- [4] Taylor, W. (2006). Good Design Impedes Bad Vibrations. RSES Journal, 27-28.